3D REAL-TIME IN SITU CHARACTERISATION, DIRECT NUMERICAL SIMULATION, AND ANALYTICAL MODELLING OF FIBRE KINEMATICS IN DILUTE NON-NEWTONIAN FIBRE SUSPENSIONS DURING CONFINED COMPRESSION

L. Laurencin[1,2,3,4], P.J.J. Dumont[3], L. Orgéas[1], P. Laure[2,5], S. Rolland du Roscoat[1], S. Le Corre[6] and L. Silva[4]

[1]Univ. Grenoble Alpes, CNRS, Grenoble INP, 3SR Lab, F-38000 Grenoble, France
Email: laurent.orgeas@3sr-grenoble.fr
[2]Univ. Côte d'Azur, CNRS, Lab. J.A. Dieudonné, Parc Valrose F-06000 Nice, France
Email: patrice.laure@unice.fr
[3]Univ. Lyon, LaMCoS, INSA-Lyon, CNRS UMR5259, F-69621, Lyon, France
Email: pierre.dumont@insa-lyon.fr
[4] École Centrale de Nantes, ICI, 1 rue de la Noë F-44000 Nantes, France
[5] PSL, CNRS, MINES ParisTech, CEMEF, 06904 Sophia Antipolis, France
[6] Univ. Nantes, LTN, La Chantrerie, rue Christian Pauc - CS 50609, 44306, Nantes, cedex 3, France

Keywords: Short Fibre-Reinforced composites; Fibre Suspension; X-ray microtomography, Direct Numerical Simulation; Confinement; Jeffery's Model

Abstract
The physical and mechanical properties of short fibre-reinforced polymer composites depend on the geometry, content, distribution and orientation of fibres which drastically evolve during composite forming. Short fibre composites can be seen as non-Newtonian fibre suspensions. Within the mould cavities these suspensions are subject to confined flow conditions. Unfortunately, the flow-induced microstructures of these suspensions cannot be well predicted by current rheological models which limits the development of short fibre composites. Hence, in this study, lubricated compression. 3D real-time and in situ observations of the compression of non-Newtonian dilute fibre suspensions were conducted using fast X-ray microtomography. These experiments enabled fast and in situ 3D imaging of the translation and rotation of fibres in the suspending fluid. In addition these experiments were simulated using a multi-domain Finite Element code. Often, the Jeffery's equations agree well with the experimental and numerical data except for fibres closed to the compression platens for which important deviations were observed with faster simulated and experimental fibre rotations. A simple dumbbell approach was also proposed to account both for the non-Newtonian rheology of the suspending fluid and confinement effects. Despite its simplicity, this model allows a good description of both simulation and experimental results.

1. Introduction

Short fibre reinforced polymer composites are increasingly used for the fabrication of semi-structural and structural parts for the automotive, aeronautic and electrical fields because of their interesting specific physical and mechanical properties and their cost-efficient forming. These materials have fibre volume fractions ϕ that range from 0.005 to 0.5 and fibre aspect ratios $\beta = l/d$ from 5 to 1000 (d and l being the typical fibre diameter and length, respectively).

The strong coupling phenomena between the rheology and the microstructure (fibre volume fraction, fibre orientation) of these suspensions drastically alter the end-use properties of short-fibre composites

[1-3]. During forming, these materials behave as highly concentrated fibre suspensions and exhibit complex rheology. These suspensions are subject to confined flow conditions within the mould cavities with typical thickness h of the same order of magnitude as the size of the fibre length l, i.e, with a confinement parameter $C^* = h/l = O(1)$ [4-6]. These flow situations lead to interactions between fibres and solid boundaries that alter the fibre kinematics. The aforementioned effects should be considered to simulate the processing of short fibre-reinforced polymer composites. But they are still not very well-understood because it is difficult to properly observe the flow mechanisms at the fibre scale.

Fibre kinematics under various flow have been widely studied. Jeffery's theory [7] assumes that the translation of an ellipsoidal particle immersed in an incompressible Newtonian fluid at low Reynolds number in an infinite domain is an affine function of the macroscale velocity gradient. In the case of a cylindrical fibre, the evolution of the unit tangent vector $\boldsymbol{p} = \sin\theta\cos\varphi\,\mathbf{e}_1 + \sin\theta\sin\varphi\,\mathbf{e}_2 + \cos\theta\,\mathbf{e}_3$, characterising the fibre orientation, can be predicted from the its rate $D\mathbf{p}/dt$, the macroscale vorticity tensor $\boldsymbol{\Omega}$ and the strain rate tensor $\boldsymbol{D}$:

$$D\boldsymbol{p}/dt = \boldsymbol{\Omega}\boldsymbol{p} + \lambda(\boldsymbol{D}\boldsymbol{p} - (\boldsymbol{p}\cdot\boldsymbol{D}\boldsymbol{p})\boldsymbol{p}) \text{ with } \lambda = 1-(16.35\ln\beta)/(4\pi\beta^2) \quad (1)$$

where λ is a shape factor expressed by Brenner for cylindrical fibres [8]. The relevance of Jeffery's model was experimentally confirmed by several authors [9-12], mostly under shear flow. Jeffery's model has largely been validated and used for dilute Newtonian fibre suspensions, i.e., when $\phi << 1/\beta^2$ [13-15].

Jeffery's model was enriched to account long range hydrodynamic fibre interactions [16-20] in semi-dilute and Newtonian fibre suspensions ($1/\beta^2 << \phi << 1/\beta$). The motions of the centres of mass of fibres are still affine functions of the macroscale velocity gradients. However, the fibre rotations are restrained thanks to a diffusion-like term that depends on the Fibre Orientation Distribution Function (FODF). In the concentrated regime, Jeffery-based models fail due to short range interactions between fibres which play a central role on the rheology of these suspensions [16, 21-23].

The aforementioned theories were established for a good scale separation with $C^* >> 1$. For confined flow conditions ($C^* = h/l = O(1)$), departures from Jeffery's trajectories and orbits were reported for fibres because they interacted with mould walls in Newtonian [24-27] and non-Newtonian suspending fluids [28]. Few models account for the effects of confinement. Using a dumbbell representation for the fibres, modifications of the Jeffery's equations [29-31] were recently proposed by considering physical contacts between rods and walls through the introduction of a contact force ensuring wall impenetrability. Confinement effects have rarely been studied in the case of non-Newtonian suspending fluids [28], and never for elongational flows.

Thus, in this study, we used real time and in situ synchrotron X-ray microtomography to measure the 3D fibre kinematics in dilute suspensions with a shear thinning fluid during confined and lubricated compression tests [32]. Besides, these experiments were modelled using both direct fibre scale numerical simulation and analytical predictions based an extension of the Jeffery's model and dumbbell approach to account both for the non-Newtonian rheology of the suspending fluid and confinement effects.

2. Materials and Methods

Original compression rheometry experiments were conducted to better understand the flow-induced phenomena in confined short-fibre suspensions. For that, we combined fast 3D X-ray microtomography (Swiss Light Source, Tomcat beamline, Villigen, Switzerland) and a specially designed compression rheometer to analyse flow-induced microstructures of suspensions with varying fibre concentrations. These suspensions consisted of elastic polymeric slender fibres (PFVD)

suspended in a non-Newtonian fluid (paraffin gel) (Figure 1). These fibre suspensions were subjected to lubricated simple compression loading at 50°C and constant velocities. The suspension flow was considered as confined due to poor scale separation, i.e., $C^* = l/h = O(1)$. Thanks to very short scanning times, 3D images of the evolving fibrous microstructures at high spatial resolution were recorded in real-time. From these original rheometry experiments, dedicated image analysis procedures were used to detect and follow the position, orientation and deformation of fibres as well as the number, position and orientation of fibre-fibre contacts [32] (Figure 2).

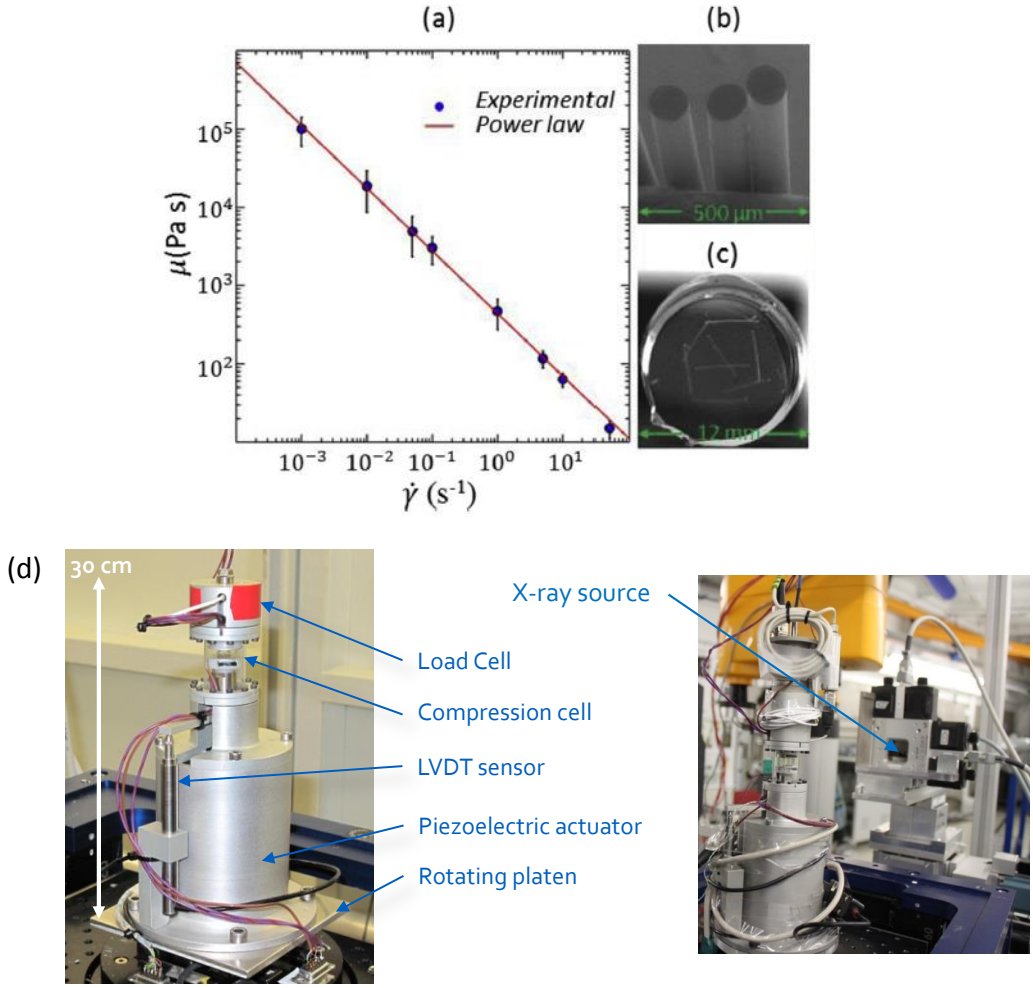

Figure 1. (a) Evolution of the shear viscosity of the hydrocarbon gel as a function of the shear rate at the testing temperature. (b) SEM micrograph showing the cut extremities of PVDF fibres. (c) Upper view of a fibre suspension sample with eight fibres. (d) Global view of the compression micro-rheometer mounted on the rotation stage of the TOMCAT beamline at the Paul Scherrer Institute (Villigen, Switzerland).

These experiments were also simulated using a dedicated finite element library, enabling an accurate description of fibre kinematics in complex suspending fluids thanks to high performance computation, levelsets and adaptive anisotropic meshing. The velocity and the pressure fields were computed by solving the Stokes equation in a cubic domain Ω composed of subdomains Ω_j made of N fibres i, the suspending fluid f, the air a and the compression platens p (Figure 3). All subdomains were embedded in a unique Eulerian mesh using the immersed volume method [33]. Levelsets were used to get implicit representation of the interfaces between the subdomains, and to define the overall viscosity μ

as a space dependent function [33, 34]. Each levelset α_j was associated with a subdomain Ω_j. In each subdomain Ω_j, the levelsets allowed its value μ_j to be associated to the overall viscosity μ, using smooth Heaviside functions.

In addition, an extended dumbbell approach (not detailed here) was proposed for the case of dilute fibre suspensions with generalised Newtonian fluids, and a proper description of contact conditions in confined situations.

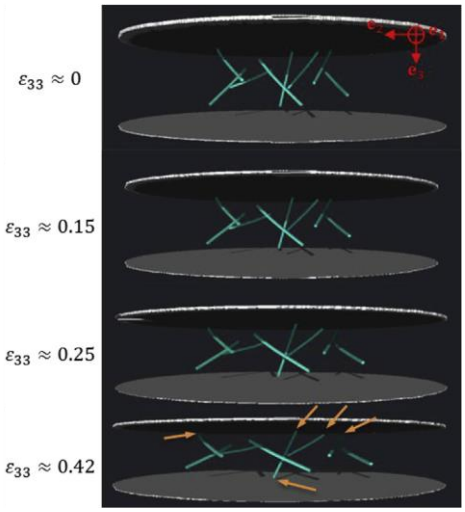

Figure 2. 3D segmented images obtained at various compression strains $|\varepsilon_{33}|$ showing the motion of the fibres of the tested sample during compression. The orange arrows point to the extremity of fibres that are very close to the compression platens. The orbits of these fibres deviate from the predictions of Jeffery's model.

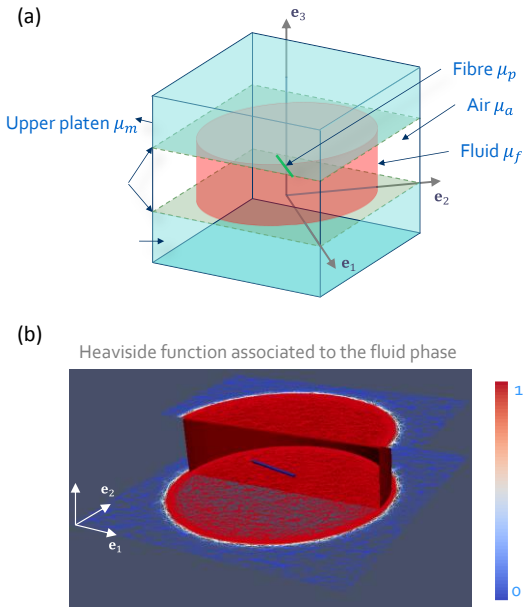

Figure 3. (a) Multi-domain approach used with the immersed domain method to simulate the lubricated compression experiments. (b) Heaviside function associated to the fluid domain.

3. Results

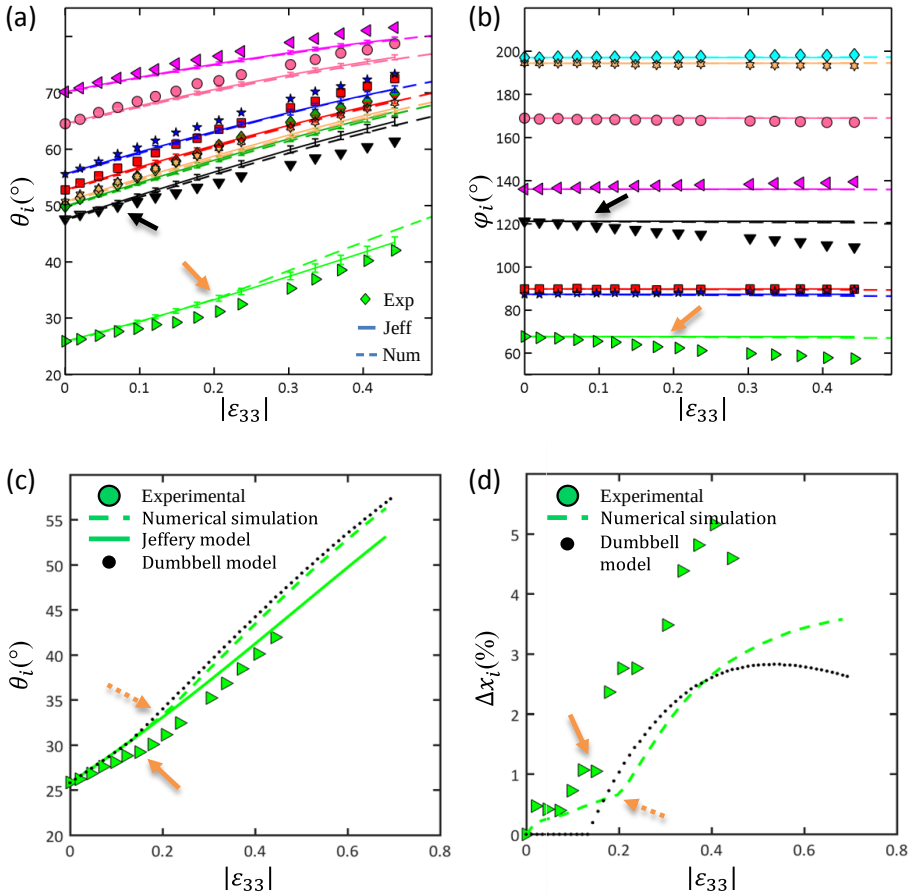

Figure 4. (a,b) Example of the compression results of a sample of dilute fibre suspension containing 8 fibres. Evolutions of the measured (marks), analytically (lines, Jeffery's model) and numerically (dashed lines) predicted evolutions for the angles θ_i (a) and φ_i (b) with the compression strain $|\varepsilon_{33}|$. Black and orange arrows denote fibres that are close (less than half one fibre diameter) and enter in contact with platen(s) during compression. (c,d) Evolutions of the angles θ_i (a,c) and the deviations $\Delta x_i^{exp} = |\boldsymbol{x}_{Gi}^{exp} - \boldsymbol{x}_{Gi}^{J}|/h_0$ and Δx_i^{num} of the fibre centre of mass (with respect to the Jeffery's predictions, h_0 being the initial thickness of the sample) (b,d) for one fibre (green triangles) in contact with the compression platens. The orange arrows (experimental: filled, numerical: dotted) denote the first contact of the considered fibre with the upper platen, and the red arrows the second with the lower platen.

Figures 4a,b show the evolution of the orientation θ_i and φ_i of the 8 fibres of a sample of dilute non-Newtonian fibre suspension during lubricated compression. The angles θ_i increased during compression while the angles φ_i were more or less constant except for some fibres indicated by balcak and orange arrows. For these fibres, the angles φ_i slightly varied and the angles θ_i increased more rapidly at given compression strains. Apart for the simulated angles φ_i for the fibres shown by the arrows, it is interesting to note that the aforementioned experimental trends were rather well-captured by the numerical simulation. The predictions of Jeffery's model were also satisfactory, except for the fibres shown by the arrows. For these fibres, the predicted angles θ_i were noticeably lower than the experimental and simulated angles. It was shown that these deviations were related neither to fibre-fibre contacts nor long range hydrodynamic interactions between fibres. Thus, the contact of these

fibres with the compression platens that were experimentally observed and simulated were probably at the origin of these deviations. When contacts with the platens occurred, both the numerical fibre orientation and deviation from the affine assumption deviated from Jeffery's prediction. This is shown in Figures 4c,d where the filled orange arrows denote the occurrence of the contacts between one the fibre with green symbols and one compression platen. Figures 4c,d show that the first contact occurred at $|\varepsilon_{33}| \sim 0.15$. It is interesting to note that these events which induced deviations from Jeffery's predictions were rather well predicted by the numerical simulation, as shown by the dotted orange arrows which denote the numerical contacts. Note also that the extended dumbbell approach which could rather well predict the occurrence of contacts for the considered fibre.

4. Conclusion

The microstructure of short fibre composites is mainly governed by the flow phenomena that occur on these materials that can be seen as non-Newtonian fibre suspensions during forming. Within this context, fast and in situ 3D imaging of the translation and rotation of fibres in non-Newtonian dilute fibre suspensions were conducted using original X-ray microtomography experiments. The fibre motions were compared with the predictions of Jeffery's model. Despite the use of a non-Newtonian suspending fluid and confined flow conditions, *i.e.*, with a gap between compression platens of the same order of magnitude than the fibre length, predictions of Jeffery's model were satisfactory if the fibres were sufficiently far from the compression platens (approximately at a distance of once to twice their diameter). Otherwise, the experimental average orientation rates were higher than Jeffery's prediction. These experiments were simulated using a multi-domain finite element code and compared with the predictions of Jeffery's model. For fibres closed to compression platens, important deviations from Jeffery's predictions were observed with faster simulated and experimental fibre rotation. Adopting the dumbbell approach, an extension of the Jeffery's model was proposed to account both for the non-Newtonian rheology of the suspending fluid and confinement effects. This model allowed a good description of simulation and experimental results.

Acknowledgments

T. Laurencin gratefully acknowledges the LabEx Tec21 (Inv. d'Avenir - grant agreement n°ANR-11-LABX-0030) for his PhD research grant. The 3SR Lab is part of LabEx Tec 21 and the Carnot Institute Polynat. We acknowledge the Paul Scherrer Institut, Villigen, Switzerland for provision of synchrotron radiation beamtime at the TOMCAT beamline of the Swiss Light Source.

References

[1] S. Advani, of Composite Materials Series, Flow and Rheology in Polymer, Composites Manufacturing, vol. 10, Elsevier, 1994.
[2] J.L. Thomasson, M.A. Vlug, Influence of fibre length and concentration on the, properties of glass fibre-reinforced polypropylene: 1. Tensile and flexural, modulus, *Composites Part A* 27A (1996) 477-484.
[3] S. Fu, Y. Mai, Thermal conductivity of mislaligned short-fiber reinforced polymer composites, *J. Appl. Polym. Sci.* 88 (2003) 1497-1505.
[4] H. Diamant, Hydrodynamic interaction in confined geometries, *J. Phys. Soc. Jpn*, 78 (2009) 041002.
[5] R. Schiek and E. Shaqfeh, Oscillatory shear of a confined fiber suspension, *J. Rheol.*, 41 (1997) 445-466.
[6] B. Snook, E. Guazzelli, J. Butler, Vorticity alignment of rigid fibers in an oscillatory shear flow: Role of confinement, *Phys. Fluids*, 24 (2012) 121702.
[7] G. B. Jeffery, The motion of ellipsoidal particles immersed in a viscous fluid, *Proc. Roy. Soc. A* 102 (1922) 161–179.

[8] H. Brenner, Rheology of a dilute suspension of axisymmetric Brownian particles, *Int. J. Multiphase Flow*, 1 (1974) 195–341.
[9] A. Binder, The motion of cylindrical particles in viscous flow, *J. Appl. Phys.*, 10 (1939) 711 – 713.
[10] M. P. Petrich, D. L. Koch, C. Cohen, An experimental determination of the stress-microstructure relationship in semi-concentrated fiber suspensions, *J Non-Newt. Fluid Mech.*, 95 (2000) 101-133.
[11] G. Taylor, The motion of ellipsoidal particles in a viscous fluid, *Proc. R. Soc. A* 103 (1923) 58–61.
[12] B. J. Trevelyan, S. G. Mason, Particle motions in sheared suspensions I. Rotations, *J. Colloid Sci.*, 6 (1951) 354–367.
[13] E. Anczurowski, S. G. Mason, Particle motions in sheared suspensions XXIV. Rotation of rigid spheroids ans cylinders, *Trans. Soc. Rheol.*, 12 (1968) 209.
[14] M. Rahnama, D. L. Koch, C. Cohen, Observations of fiber orientation in suspensions subjected to planar extensional flows, *Phys. Fluids*, 7 (1995) 1811–1817,.
[15] S. Sinha-Ray, K. Fezzaa, A. L. Yarin, The internal structure of suspensions in uniaxial elongation, *J. Appl. Phys.*, 113 (2013) .
[16] R. S. Bay, Fiber Orientation in Injection Molded Composites: A Comparison of Theory End Experiments. PhD thesis, University of Illinois, USA, 1991.
[17] F. Folgar, C. L. Tucker, Orientation behavior of fibers in concentrated suspensions, *J. Reinf. Plast. Compos.*, 3 (1984) 98-118.
[18] D. L. Koch, A model for orientational diffusion in fiber suspensions, *Phys. Fluids*, 7 (1995) 2086-2088.
[19] N. Phan-Thien, X. J. Fan, R. I. Tanner, R. Zheng, Folgar-Tucker constant for a fibre suspension in a Newtonian fluid, *J. Non-Newt. Fluid Mech.*, 103 (2002) 251-260.
[20] J. Phelps and C. Tucker, An anisotropic rotary diffusion model for fiber orientation in short- and long-fiber thermoplastics, *J. Non-Newt. Fluid Mech.*, 156 (2009) 165-176.
[21] P. Dumont, J.-P. Vassal, L. Orgéas, V. Michaud, D. Favier, J.-E. Månson, Processing, characterization and rheology of transparent concentrated fibre bundle suspensions, *Rheol. Acta*, 46 (2007) 639-651.
[22] P.J.J. Dumont, S. Le Corre, L. Orgéas, D. Favier, A numerical analysis of the evolution of bundle orientation in concentrated fibre-bundle suspensions, *J. Non-Newt. Fluid Mech.*, 160 (2009) 76–92.
[23] T.H. Le, P.J.J. Dumont, L. Orgéas, D. Favier, L. Salvo, E. Boller, X-ray phase contrast microtomography for the analysis of the fibrous microstructure of SMC composites, *Composites Part A*, 39 (2008), 91-103.
[24] A. Carlsson, F. Lundell, D. Soderberg, The wall effect on the orientation of fibres in a shear flow, in Annual Transactions of the Nordic Rheology Society, 2006.
[25] R. Holm, Shear influence on fibre orientation, *Rheol. Acta*, 46 (2007) 721-729.
[26] K. Moses, S. Advani, A. Reinhardt, Investigation of fiber motion near solid boundaries in simple shear flow, *Rheol. Acta*, 40 (2001) 296-306.
[27] W. Russel, E. Hinch, Rods falling near a vertical wall, *J. Fluid Mech.*, 83 (1977) 273-287.
[28] C. Stover, C.Cohen, The motion of rodlike particles in the pressure driven flow between two plates, *Rheol. Acta*, 29 (1990) 192-203.
[29] A. Ozolins, U. Strautins, Simple models for wall effect in fiber suspension flows, *Math. Model. Anal.*, 19, (2014) 75-84.
[30] M. Perez, A. Scheuer, E. Abisset-Chavanne, F. Chinesta, R. Keunings, A multi-scale description of orientation in simple shear flows of confined rod suspensions, *J. Non-Newt. Fluid Mech.*, 233 (2016) 61-74.
[31] A. Scheuer, E. Abisset-Chavanne, F. Chinesta, R. Keunings, Second gradient modelling of orientation development and rheology of dilute confined suspension, *J. Non-Newt. Fluid Mech.*, 237 (2016) 54-64.
[32] T. Laurencin, L. Orgéas, P.J.J. Dumont, S. Rolland du Roscoat, P. Laure, S. Le Corre, L. Silva, R. Mokso, M. Terrien, 3D real-time and in situ characterisation of fibre kinematics in dilute non-

newtonian fibre suspensions during confined and lubricated compression flow, *Compos. Science Technol.*, 134 (2016) 258-266.
[33] T. Coupez, H. Digonnet, E. Hachem, P. Laure, L. Silva, and R. Valette, Multidomain Finite Element Computations: Application to Multiphasic Problems, in Arbitrary Lagrangian-Eulerian and Fluid-Structure Interaction. Numerical Simulation. Eds. M. Souli, D.J. Benson, Wiley, 2010.
[34] S. Osher, J. Sethian, Front propagating with curvature-dependent speed. algorithm based on Hamilton-Jacobi formulations, *J. Comput. Phys.*, 79 (1988) 12-49.